

Article

# Carbothermal Reduction Nitridation of Fly Ash, Diatomite and Raw Illite: Formation of Nitride Powders with Different Morphology and Photoluminescence Properties

Kuizhou Dou, Yinshan Jiang, Bing Xue, Cundi Wei \* and Fangfei Li \*

Key Laboratory of Automobile Materials, Ministry of Education, and Department of Materials Science and Engineering, Jilin University, 5988 People's Avenue, Changchun 130025, China; doukuizhou@163.com (K.D.); jlujiangyinshan@163.com (Y.J.); xuebing2011@jlu.edu.cn (B.X.)

\* Correspondence: weicundi\_jlu@163.com (C.W.); lifangfei\_jlu@163.com (F.L.)

Received: 9 April 2020; Accepted: 18 May 2020; Published: 20 May 2020



**Abstract:** Rare-earth-doped SiAlON and Si<sub>3</sub>N<sub>4</sub> materials from aluminosilicate starting materials have been reported to show superior photoluminescence (PL) properties. Three different starting materials, including pulverized coal furnace fly ash, diatomite and raw illite, were used for synthesis of nitride materials. The phase and morphology evolution of these products were carefully monitored at the low temperature range of 1350 °C to 1450 °C by X-ray diffraction (XRD), scanning electronic microscopy (SEM) and Fourier-transform infrared spectroscopy (FT-IR). The PL properties of Eu-doped nitride products were also comparatively characterized. The results show that the type of starting material affects the phase composition and the photoluminescence properties of products. The existence of aluminum and alkali metals could effectively promote nitridation reactions. Aluminum in the starting materials led to the formation of different aluminum-rich nitride phases. Thus, β-SiAlON could be achieved at a much lower temperature (1350 °C) using raw illite or fly ash containing the proper amount of aluminum. Additionally, excess aluminum led to the formation of corundum and 15R-SiAlON. The products from pulverized coal furnace fly ash had more prismatic particles, and the products from diatomite had more fibrous particles. With the progress of the nitridation process, the fibers were increased, becoming longer and straighter, and the prismatic particles were more obvious. The presence of aluminum in the starting materials led to a blue shift in the photoluminescence spectrum.

**Keywords:** nitrides; fly ash; carbothermal reduction; nitridation; optical properties

## 1. Introduction

SiAlON materials have attracted great attention due to their reliable mechanical strength and significant structural, thermal and chemical stability during application [1,2]. Rare-earth-doped SiAlON materials are potential phosphors, due to their reported photoluminescence (PL) properties and the superior stabilities mentioned above. α-SiAlONs have been found to generate efficient luminescence [3–8]. While only a few studies have focused on β-SiAlONs, the luminescence mechanism needs further study and many details remain unclear [9].

The starting materials for production of SiAlON material can be highly purified chemical reagents [9–16], natural minerals [17–20] and solid waste [21–24]. In our previous study, we reported that β-SiAlON multiphase phosphors can be prepared from fly ash acid slag, which can be seen as a new solid waste [25]. Because fly ash is rich in silicon and aluminum, it is very suitable for preparation of SiAlON, whether through acid dissolution or not [26,27]. J.E. Gilbert et al reported that high-C fly ashes

could be used to synthesize  $\beta$ -SiAlON at 1500 °C [24]. Tao Jiang et al. reported that titania-bearing blast furnace slag and bauxite chamote could be used to synthesize (Ca, Mg)  $\alpha'$ -SiAlON [28]. Suitable solid waste could be recycled and reused as a new resource with low cost and low pollution.

Previous studies have indicated that, as a starting material for synthesis of SiAlON materials, natural minerals and solid waste can efficiently reduce the synthesis temperature and simplify the synthesis process [17–25]. However, the influence of different Si and Al sources has rarely been studied, especially for the synthesis of  $\beta$ -SiAlON materials. Yun Tang et al. [29] reported that slag, glass and minerals were compared as starting materials for synthesis of SiAlON materials. The results showed that the carbothermal reduction nitridation (CRN) processes are similar and the phase transformation steps are the same. Mikinori Hotta et al. [30] reported that nanosized amorphous, sub-micron-sized amorphous and micron-sized crystalline SiO<sub>2</sub> powders could be used to obtain Ca- $\alpha$  SiAlON. They reported that the nitridation process was similar irrespective of the difference in starting materials. In order to study the influence of different Si and Al sources, the Al:Si ratios in the starting materials should be different enough. The PL properties of the products from different starting materials need to be researched because of their potential phosphor applications.

In this work, three different starting materials with various Al:Si ratios, including pulverized coal furnace fly ash, diatomite and raw illite, providing different Si and Al sources, were used as starting materials for the synthesis of SiAlON or Si<sub>3</sub>N<sub>4</sub> (because of a lack of Al source in diatomite) materials. Among them, diatomite and raw illite are natural minerals, both of which are rarely reported as starting materials for SiAlON or Si<sub>3</sub>N<sub>4</sub>, and one of which is solid waste. Nitride phosphors were obtained by Eu doping and their phase and morphology evolutions during the CRN reaction were investigated. The PL properties of the different phosphors were researched and a comparison was made. The influences of different Si and Al sources were determined.

## 2. Materials and Methods

The pulverized coal furnace fly ash used for this study was obtained from Guohua Power Plant, Xuejiawan Town, Zhungeer County, Ordos City, Inner Mongolia, China. The diatomite was obtained from Linjiang City, Jilin Province, China. The raw illite used for this study was obtained from Antu County, Jilin Province, China. Carbon black (model N550, oil absorption 2.01, Jilin Petrochemical Co. Ltd.) was the carbon source in this study. Eu<sub>2</sub>O<sub>3</sub> (99.99 %, Sinopharm Chemical Reagent Co. Ltd.) was used to prepare phosphors. Starting materials with molar ratio C:Si = 3.02 with Eu doping content 0.05 were weighed and mixed in a mortar [25]. Then, the starting powders were placed in alumina boats positioned in a box type furnace. The reaction temperatures of different samples were 1350 °C, 1400 °C and 1450 °C. Then, the temperature was maintained for 3 h and 6 h under nitrogen flow (flow rate of 2 L/min), respectively. The samples were cooled to room temperature in the furnace and characterized at room temperature.

The phase composition of the products was characterized by X-ray diffraction (XRD, DX-2700, Dandong, China). The XRD (Cu K $\alpha$ 1 radiation, 35 kV and 25 mA) patterns were obtained by scanning from 10° to 80°. The step size was 0.1 °/s. The sampling time was 0.5 s and the data point interval (the step width of scanning) was 0.05°. The Fourier-transform infrared spectroscopy (FT-IR) of samples was determined by a Fourier-transform infrared spectrometer (NICOLET 380, Fitchburg, Wisconsin, USA) in the range of 400–1300 cm<sup>-1</sup> with a spectral resolution of 2 cm<sup>-1</sup>. The photoluminescence properties were measured by a fluorescence spectrophotometer (F-380, Tianjin, China). The morphology of the products was characterized by scanning electronic microscopy (SEM, S-570 and JSM-IT300, Tokyo, Japan). The chemical composition of the product was analyzed by energy-dispersive spectroscopy (EDS, JED-2300, Tokyo, Japan).

### 3. Results and Discussion

#### 3.1. Analysis of Experimental Raw Materials

Pulverized coal furnace fly ash is the discharged solid waste of coal combustion, which has a large amount of amorphous phase composed of silica and alumina. Natural diatomite contains the highest content of amorphous  $\text{SiO}_2$  and the lowest Al:Si ratio, while raw illite is mainly composed of crystalline aluminosilicate phase, which has the highest alkali metal content. In terms of loss on ignition (LOI) caused by combustible organic matter and absorbed water, pulverized coal furnace fly ash is relatively low and close to raw illite.

The chemical compositions of these starting materials are listed in Table 1, and were detected by methods of chemical analysis for silicate rocks (Chinese GB/T 14506–2010). In terms of chemical composition, fly ash and raw illite are mainly composed of silica and alumina, while diatomite is mainly composed of silica. Variations of Al:Si ratio in the starting materials will affect the forming process of aluminum-containing products such as corundum and SiAlON during CRN synthesis. From the perspective of alkali metal oxides which have greatest influence on thermal reactivity, raw illite displays the highest content of potassium oxide, indicating the lowest melting point of the resultant mixture. This means that differences in the chemical composition of the starting materials will greatly affect the thermal reactivity, morphology, phase forming and transition process during CRN.

**Table 1.** Composition of starting materials (mass fraction, %).

Composition	Fly Ash	Diatomite	Raw Illite
$\text{SiO}_2$	40.25	87.85	70.41
$\text{Al}_2\text{O}_3$	49.61	2.40	16.15
$\text{TiO}_2$	1.98	0.11	0.39
CaO	1.70	0.29	1.09
MgO	0.22	0.34	0.61
$\text{Fe}_2\text{O}_3$	1.36	1.02	1.03
$\text{K}_2\text{O}$	0.38	0.43	5.15
$\text{Na}_2\text{O}$	0.07	0.17	0.03
LOI	3.27	7.37	3.50

The crystalline structure analyzed by the XRD method for different starting materials is shown in Figure 1. The major phases of the pulverized coal furnace fly ash are mullite ( $\text{Al}_6\text{Si}_2\text{O}_{13}$ ), corundum ( $\text{Al}_2\text{O}_3$ ) and amorphous silica phase. These correspond to the high content of alumina in the chemical composition (Table 1). Diatomite is mainly composed of an amorphous phase, with no other crystalline phase except for quartz. The crystalline phases of raw illite are mainly composed of quartz and illite. The source of silicon in synthesizing SiAlONs is mainly the amorphous phase and mullite in fly ash, the amorphous phase and quartz in diatomite, and the quartz and illite in raw illite. This means that differences in the crystalline structure of starting materials will also greatly affect the phase forming of SiAlONs.

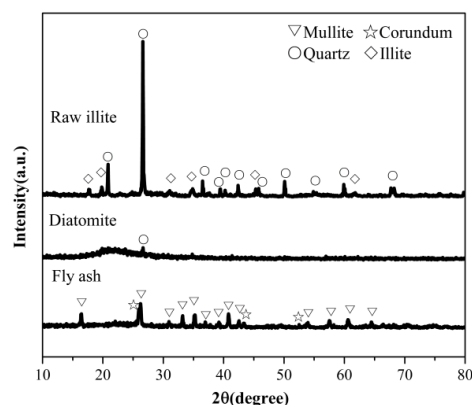


**Figure 1.** XRD patterns of various starting materials.

### 3.2. The Effect of the Si Sources on the Phase Composition of Products

During CRN calcination, these raw materials are partly reduced and nitrified. The XRD patterns of the products obtained from different starting materials are shown in Figure 2. The phase compositions of the products are identified by their XRD patterns [6,8–11,25,29]. At 1350 °C, the intermediate phase  $\text{Si}_2\text{N}_2\text{O}$  exists in the products of the pulverized coal furnace fly ash, diatomite and raw illite. This means that  $\text{Si}_2\text{N}_2\text{O}$  exists at all of the initial stages of carbothermal reduction and nitridation reaction, regardless of the various initial chemical compositions and crystal structures of silicon sources. Although the nitridation process has started at 1350 °C, the  $\beta$ -SiAlON phase only exists in the products of the pulverized coal furnace fly ash and raw illite, both of which are rich in alumina. There is no  $\text{Si}_3\text{N}_4$  phase in the product of the diatomite. Therefore, it implies that, in our CRN system, the forming temperature of  $\beta$ -SiAlON is lower than that of the  $\text{Si}_3\text{N}_4$  phase, and rich alumina species in fly ash and raw illite improve the nitridation process to form SiAlONs. Considering that a large amount of silicon carbide is produced in diatomite instead of  $\text{Si}_3\text{N}_4$ , the carbonization process must take precedence over the nitridation process in a nitrogen atmosphere for diatomite, even when part of the silicon carbide acts as the intermediate product of the nitridation process. Mullite and corundum from the starting materials remain in the 1350 °C products of fly ash. Meanwhile, quartz from diatomite and raw illite is completely converted into cristobalite and other phases below 1350 °C.

At 1400 °C, the amount of  $\text{Si}_2\text{N}_2\text{O}$  decreases sharply and only remains in the products of pulverized coal furnace fly ash due to its high Al:Si ratio. As an intermediate nitride product at low temperatures, the vanishing of  $\text{Si}_2\text{N}_2\text{O}$  indicates that the nitridation process is completed. Thus, more  $\beta$ -SiAlON and SiC phase exist in the products. The phases in the products from illite mineral are basically pure  $\beta$ -SiAlON and a small amount of SiC, which can be regarded as an almost complete nitriding process. As for diatomite, SiC phase in the products is greatly reduced, and replaced by  $\text{Si}_3\text{N}_4$  with two structures:  $\alpha$ - $\text{Si}_3\text{N}_4$  and  $\beta$ - $\text{Si}_3\text{N}_4$ . These two  $\text{Si}_3\text{N}_4$  phases with different structures appear almost at the same time.

At 1450 °C, in addition to the phases in the products at 1400 °C, pulverized coal furnace fly ash also produces aluminum-rich nitride phase 15R-SiAlON ( $\text{SiAl}_4\text{O}_2\text{N}_4$ ). In the products of pulverized coal furnace fly ash, corundum is always accompanied. That means aluminum is excessive in the chemical composition of pulverized coal furnace fly ash corresponding to  $\beta$ -SiAlON. There is no obvious evidence of AlN phase in XRD patterns of products, and, even if formed, they are below detectable limits, similar to the result in [31]. For diatomite at 1450 °C, the resultant phases are the same as that of 1400 °C. Illite mineral produced a small amount of corundum phase on the basis of  $\beta$ -SiAlON and a small amount of SiC.

To sum up, the aluminum species in the starting materials promote the nitriding reaction. Thus, the initial forming temperature of  $\beta$ -SiAlON is lower than silicon nitride, and aluminum-rich nitride phase will be formed at higher temperature, 1450 °C. The products of different raw materials are all  $\beta$ -SiAlON phase, while  $\alpha$ - $\text{Si}_3\text{N}_4$  and  $\beta$ - $\text{Si}_3\text{N}_4$  are produced at almost the same time. The higher alkali metal content in the raw materials, such as  $\text{K}_2\text{O}$ , will promote the production of SiAlON at lower temperatures, although no independent phase or new phase different from other aluminosilicate starting materials is observed.

The FT-IR spectra of the products obtained from different starting materials are shown in Figure 3. At 1350 °C, the spectrum of the products of pulverized coal furnace fly ash does not exhibit the characteristic absorption at  $1100\text{ cm}^{-1}$  of the Si-O bond [32]. The spectrum of the products of raw illite does not obviously exhibit characteristic absorption at  $950\text{ cm}^{-1}$  of the N-Si-O bond [32], which corresponds to the complete nitridation reaction. The peaks at  $1100\text{ cm}^{-1}$  are generally assigned to the characteristic absorption of the Si-O bond [32]. The peaks at 1000, 950, 900 and  $540\text{ cm}^{-1}$  are generally assigned to the characteristic absorption of N-Si-O bond. The peaks at  $490\text{ cm}^{-1}$  are generally assigned to the characteristic absorption of the Si-N bond [33]. The peaks at  $460\text{ cm}^{-1}$  are generally assigned to the characteristic absorption of the Al-O bond [32]. The peaks at  $430\text{ cm}^{-1}$  are generally assigned to the characteristic absorption of the Si-O bond [32,34].

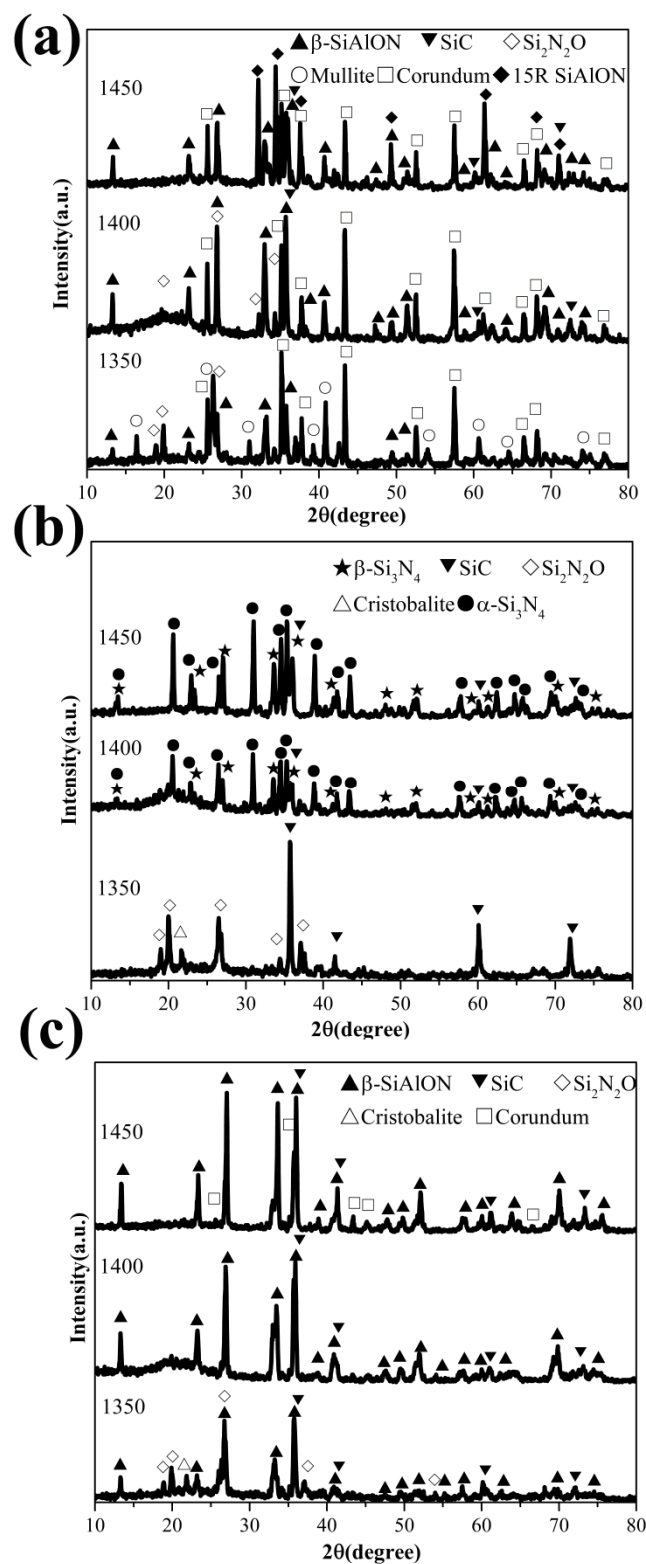


**Figure 2.** XRD patterns of the products obtained from different starting materials: (a) pulverized coal furnace fly ash (b) diatomite (c) raw illite.

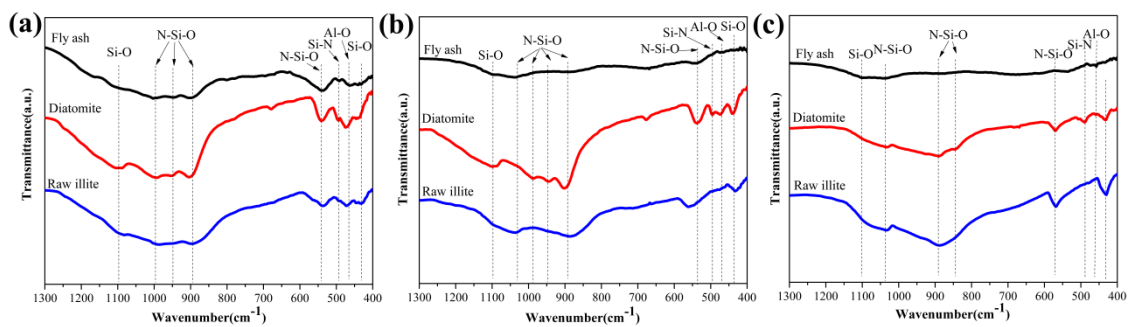


**Figure 3.** FT-IR spectra of the products obtained from different starting materials (a) 1350 °C (b) 1400 °C (c) 1450 °C.

At 1400 °C, the FT-IR spectrum of the products of raw illite does not exhibit characteristic absorption at  $1100\text{ cm}^{-1}$  of the Si-O bond [32]. The characteristic absorption of the N-Si-O bond at  $950\text{ cm}^{-1}$  only exists in the products of diatomite [32]. It corresponds to the fact that the nitridation reaction of the diatomite with less impurity is not easy. The peaks at  $490\text{ cm}^{-1}$ , assigned to  $\alpha\text{-Si}_3\text{N}_4$ , do not exist in the products of pulverized coal furnace fly ash and raw illite, consistent with the XRD results. For diatomite, the characteristic absorption of the Si-N bond at  $490\text{ cm}^{-1}$  indicates the forming of  $\alpha\text{-Si}_3\text{N}_4$  [33]. The existence of the characteristic absorption at  $460\text{ cm}^{-1}$  and the disappearance of the characteristic absorption at  $430\text{ cm}^{-1}$  is caused by the larger amount of aluminum and the lower amount of silicon in the products of pulverized coal furnace fly ash [33,34].

At 1450 °C, the characteristic absorption at  $1100\text{ cm}^{-1}$  in the products of pulverized coal furnace fly ash appears again, which is assigned to the 15R SiAlON phase considering the XRD results. The peaks of the N-Si-O bond at  $950\text{ cm}^{-1}$  in all products disappears, indicating the completed nitridation reaction at 1450 °C. The Si-N peaks at  $490\text{ cm}^{-1}$  do not exist in the products of pulverized coal furnace fly ash and raw illite, and only appear in diatomite samples. The disappearance of the  $900\text{ cm}^{-1}$  peak in the pulverized coal furnace fly ash sample may also be related to the forming competition between the 15R SiAlON phase and  $\beta\text{-SiAlON}$  phase during CRN.

### 3.3. The Effect of the Holding Time on the Phase Composition of Products

The XRD patterns of the products obtained from different starting materials with different holding times are shown in Figure 4. As shown, insufficient holding time leads to an incomplete nitridation reaction, and the  $\text{Si}_2\text{N}_2\text{O}$  is an important nitridation intermediate. Among these, diatomite is the most affected, whose XRD patterns are greatly changed with an increase in holding time. The main crystalline phase in the products of diatomite is cristobalite when the holding time is insufficient.  $\beta\text{-SiAlON}$  phase is obtained in the products of pulverized coal furnace fly ash and raw illite, and slightly increases with holding time. This indicates that the aluminum species in the starting material promote the nitridation process and help to obtain SiAlON phases rather than  $\text{Si}_3\text{N}_4$ , although SiAlON has a similar structure to  $\text{Si}_3\text{N}_4$ . When the holding time of illite is insufficient (3h), cristobalite is observed, indicating that the aluminum in raw illite is not excessive for the process of SiAlON formation by nitridation. X-SiAlON is observed in 3 h products of pulverized coal furnace fly ash, indicating that high aluminum content in fly ash will form a high-aluminum phase, even when nitridation is uncompleted.

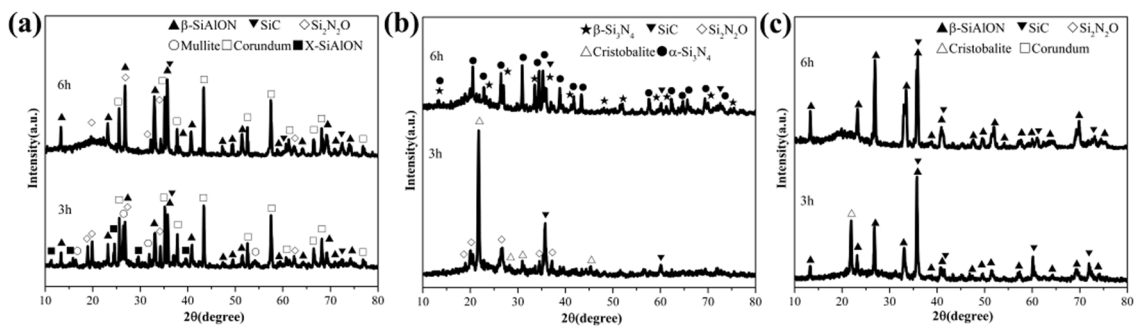


**Figure 4.** XRD patterns of the products obtained from different starting materials with different holding times at 1400 °C (a) pulverized coal furnace fly ash (b) diatomite (c) raw illite.

### 3.4. The Effect of the Si Sources on the Photoluminescence Properties of Products

The photoluminescence spectra of the products obtained from different starting materials are shown in Figure 5. The photoluminescence excitation spectra of the products obtained from different starting materials at 1350 °C, 1400 °C and 1450 °C are shown in Figure 5a–c, respectively. The photoluminescence emission spectra of the products obtained from different starting materials at 1350 °C, 1400 °C and 1450 °C are shown in Figure 5d–f, respectively. The full width of half maximum (FWHM) values of the excitation spectra of the products obtained from fly ash, diatomite and raw illite at 1350 °C are approximately 97, 80 and 99 nm respectively. The FWHM values of the excitation spectra of the products obtained from fly ash, diatomite and raw illite at 1400 °C are approximately 124 nm, 102 nm and 114 nm, respectively. The FWHM values of the excitation spectra of the products obtained from fly ash, diatomite and raw illite at 1450 °C are approximately 121 nm, 120 nm and 119 nm, respectively. The FWHM values of the emission spectra of the products obtained from fly ash, diatomite and raw illite at 1350 °C are approximately 92 nm, 93 nm and 111 nm, respectively. The FWHM values of the emission spectra of the products obtained from fly ash, diatomite and raw illite at 1400 °C are approximately 85 nm, 107 nm and 127 nm, respectively.

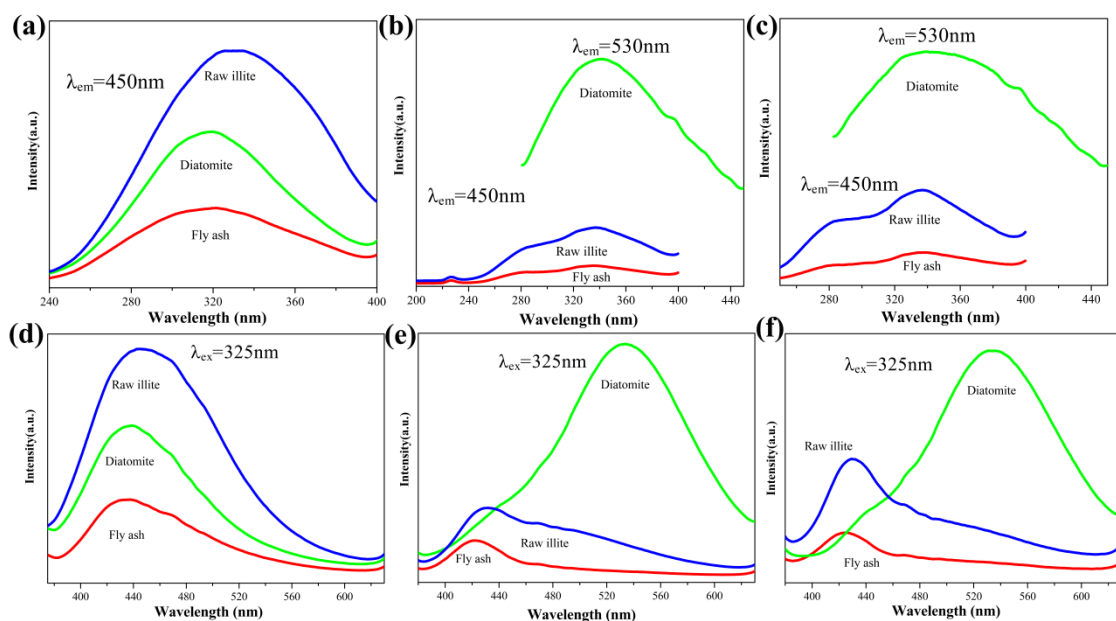


**Figure 5.** Photoluminescence excitation spectra of the products obtained from different starting materials (a) 1350 °C (b) 1400 °C (c) 1450 °C and emission spectra of the products obtained from different starting materials (d) 1350 °C (e) 1400 °C (f) 1450 °C.

The FWHM values of the emission spectra of the products obtained from fly ash, diatomite and raw illite at 1450 °C are approximately 140, 107 and 146 nm, respectively. At 1350 °C, the sample of raw illite displays the strongest luminescence. This may be related to the priority of  $\beta$ -SiAlON in the products of raw illite. In all temperature ranges, the photoluminescence intensities of the products from pulverized coal furnace fly ash are the weakest, which is probably related to the existence of the corundum phase. As revealed by XRD analysis, in the product system from pulverized coal furnace fly ash, corundum is the exact phase which always exists in all temperature ranges and differs from the phases of other starting materials. At 1400 °C and 1450 °C, the photoluminescence intensities of the products from diatomite rise sharply, and are much higher than those of the other two systems. This indicates that the photoluminescence intensity of  $\text{Si}_3\text{N}_4$  is higher than that of the other two systems. From the above two aspects, although aluminum promotes the nitridation process from the point of phase evolution, it can be considered that the existence of aluminum has a negative impact on the photoluminescence performance.

According to peak position analysis of the photoluminescence excitation spectra, the samples were excited at 325nm. According to the peak position analysis of the photoluminescence emission spectra, the peak positions of the product of all of the samples calcined at 1350 °C are close to 435 nm, approximately, attributing to blue spectral range. When the CRN temperature increases to 1400 °C, the peak positions of the products from diatomite change significantly to the green spectral range, centered at approximately 530 nm. The result is similar to related studies [6,9,35]. Ryu et al. [6] reported  $\beta$ -SiAlON:Eu<sup>2+</sup> showed a single intense broadband emission in the range from 525 to 540 nm, and exhibited broad bands of the spectra of the Eu<sup>2+</sup> ions in the present  $\beta$ -SiAlON lattice. Zhu et al. [9] reported Eu<sup>2+</sup>-doped  $\beta$ -SiAlON phosphor emission spectra exhibited two broad bands with maxima at about 415 nm (violet) and 540 nm (green), and the broad band excitation is attributed to the  $4f^7 \rightarrow 4f^65d$  transition of Eu<sup>2+</sup>. Yu et al. [35] reported Eu-doped  $\text{Si}_3\text{N}_4$  emission spectra exhibited a broad band ranging from 500 to 700 nm, and the emission band was attributed to the allowed  $4f^65d \rightarrow 4f^7$  transition of Eu<sup>2+</sup> ion. In summary, the emission bands in our study are attributed to the allowed  $4f^65d \rightarrow 4f^7$  transition of Eu<sup>2+</sup> ion. The emission spectra of the products calcined at 1400 °C and 1450 °C from diatomite are redshifted. This is related to the change of phase composition, especially the production of two different structures of  $\text{Si}_3\text{N}_4$ . The above results imply that the photoluminescence performance of the  $\text{Si}_3\text{N}_4$  system differs from that of the SiAlON system. It can also be considered that the presence of aluminum will lead to the blue shift in the photoluminescence spectrum. The blue shift of the peaks of pulverized coal furnace fly ash and raw illite at 1400 °C and 1450 °C can be regarded as the change in the photoluminescence properties of the two systems caused by nitridation.

### 3.5. Product Morphology

SEM micrographs of the different starting materials and their typical nitridation products are shown in Figure 6. In pulverized coal furnace fly ash, there are spherical particles and irregular particles, which may affect the morphology of later products. Diatomite displays relatively complete or broken porous algal disc morphology. Raw illite has a multi-layer lamellar morphology, which is typical morphology of clay minerals.

In the products of pulverized coal furnace fly ash, many particles maintain the spherical shape at 1350 °C, and a small amount of fibers also exists, which is related to the nitridation process. But the EDS results show that these fibers are not nitrides but carbides. It is likely that the nitridation products from the silicon carbide transformation maintain the morphology of silicon carbide. At 1400 °C, the aggregations of prismatic particles increased, and the spherical products disappeared, indicating that most of the silica species from the spheres reacted in the CRN condition. Although the change in the phase composition in XRD patterns was not obvious, the nitridation process and the production of  $\beta$ -SiAlON led to the replacement of spherical particles by prismatic particles directly. At 1450 °C, with the deepening of nitridation process, the products maintain the aggregation morphology of prismatic particles and the

particle sizes obviously increase. With the increasing temperature, more  $\beta$ -SiAlON phase is formed, and the morphology of fly ash changes from a spherical to a prismatic shape.

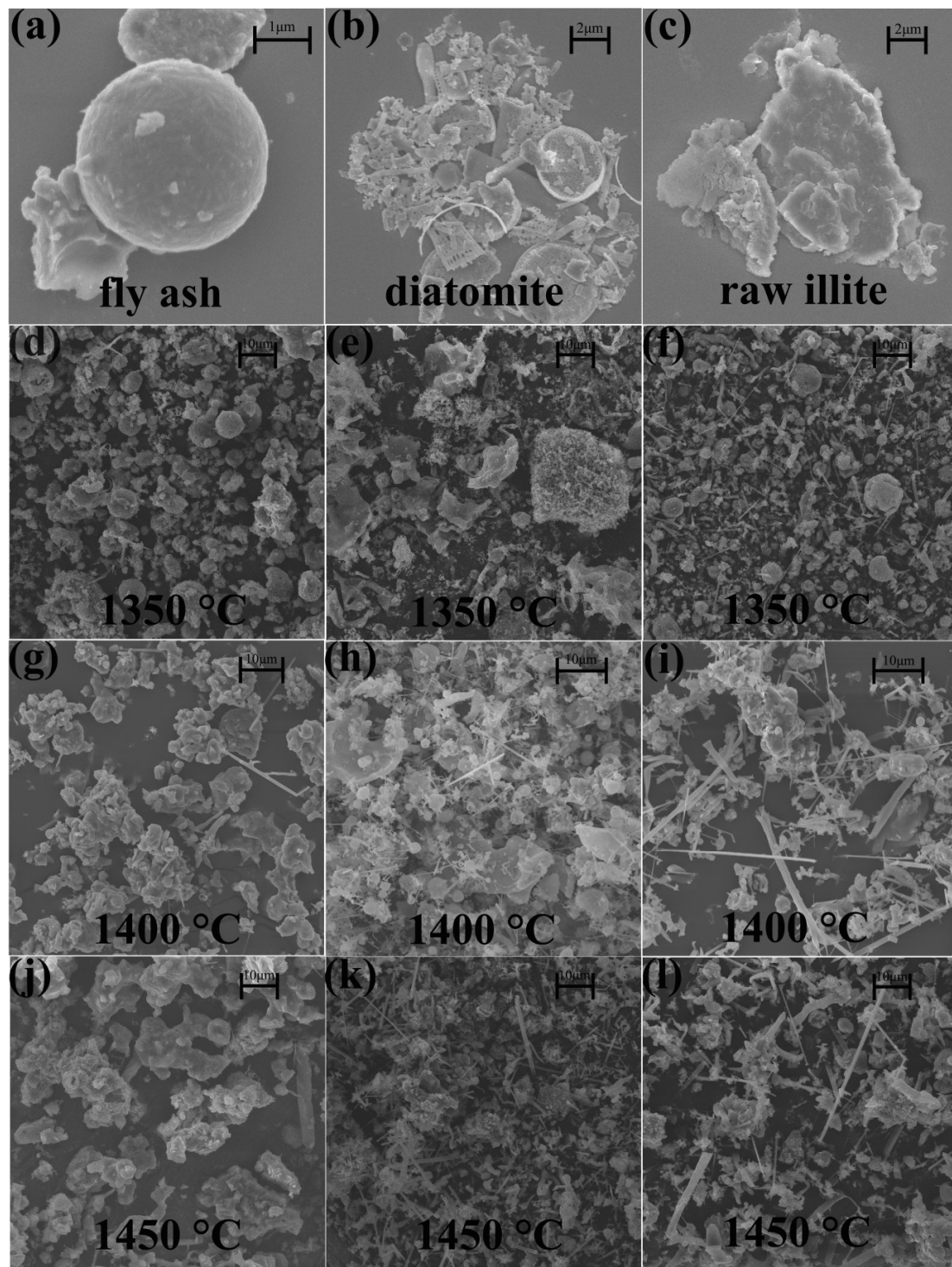


**Figure 6.** The SEM images of (a) pulverized coal furnace fly ash, (b) diatomite, (c) raw illite, (d) products from pulverized coal furnace fly ash at 1350 °C, (e) products from diatomite at 1350 °C, (f) products from raw illite at 1350 °C, (g) products from pulverized coal furnace fly ash at 1400 °C, (h) products from diatomite at 1400 °C, (i) products from raw illite at 1400 °C, (j) products from pulverized coal furnace fly ash at 1450 °C, (k) products from diatomite at 1450 °C and (l) products from raw illite at 1450 °C.

In products from diatomite, the particles are mostly tiny, agglomerated vermicular fibers and large plates at 1350 °C. At 1400 °C, the fibers grow longer and straighter than at 1350 °C. The morphologies of the products are a mixture of fibers, small spherical particles and large plates. At 1450 °C, large plates disappear in the products, and long straight fibers and their aggregations fill the field of vision. Although the phase composition of the XRD patterns remained basically unchanged, the morphology changed greatly due to the growth of fibers. With an increase in reaction temperature, diatomite particles tend to be smaller with more fibrous products from large plates.

In the products from raw illite, the morphologies are mostly fine long straight fibers and spherical particles at 1350 °C. At 1400 and 1450 °C, the morphologies of the products change a little, which are composed of larger long straight fibers and irregular particle aggregations. Additionally, the corresponding phase composition, analyzed by XRD patterns, remains basically unchanged. With an increase in reaction temperature, the product particles from natural illite become irregular aggregations from spherical particles, and the fibers become longer and straighter.

At 1350 °C, the products of pulverized coal furnace fly ash are mostly spherical in shape, and came from the starting materials, unlike the products of diatomite and raw illite. There are a few spherical particles in the products of raw illite, but the origin of these spheres differs from that of fly ash spheres. They are newly formed spheres, indicating that part of raw the illite is melted in the samples at 1350 °C due to the higher potassium content and lower melting point of the illite system. At 1400 °C, the products of pulverized coal furnace fly ash transformed into prismatic particles caused by the formation of  $\beta$ -SiAlON phase (revealed by XRD analysis), while the products of diatomite and raw illite transformed into more fibers. Revealed by XRD analysis, the fibers are  $\alpha$ -Si<sub>3</sub>N<sub>4</sub> and  $\beta$ -Si<sub>3</sub>N<sub>4</sub> phase in the system of diatomite and  $\beta$ -SiAlON phase in the system of raw illite. There are still large plate particles in the products of diatomite, and some of them are transformed into smaller spherical particles. At 1450 °C, the prismatic particles in the products of fly ash and the fibers in the products of illite grow and the intensity of PL spectra becomes stronger. The spherical particles and plate particles in the products of diatomite disappear. With the progress of the nitridation process, the morphologies of products from different silicon sources show that the fibers are increased, becoming longer and straighter, and the prismatic particles are more obvious. The growth of particles could enhance the PL properties of the products.

#### 4. Conclusions

Eu-doped nitride multiphase materials were prepared from three different Si and Al sources—diatomite, raw illite and pulverized coal furnace fly ash—by carbothermal reduction and nitridation synthesis. Different starting materials affected the phase composition and the morphology of products. Although the expected nitridation products, SiAlON and Si<sub>3</sub>N<sub>4</sub>, can be obtained at 1350 °C to 1450 °C in all of the systems, the existence of aluminum and alkali metals can effectively reduce the reaction temperature and holding time of nitridation. Starting materials containing excess aluminum, such as fly ash, may produce nitride phases with high aluminum content, such as 15R-SiAlON and X-SiAlON (Si<sub>3</sub>Al<sub>6</sub>O<sub>12</sub>N<sub>2</sub>). The different starting materials also affected the photoluminescence properties of Eu-doped products. The emission peak positions of pulverized coal furnace fly ash and raw illite are close at approximately 435 nm from 1350 °C to 1450 °C. The emission bands are attributed to the enabled  $4f^{65d} \rightarrow 4f^7$  transition of Eu<sup>2+</sup> ions in the product system. The PL spectra emission of diatomite products changes from 440 nm at 1350 °C to approximately 530 nm with the increasing calcination temperature, due to the formation of silicon nitride phase at higher temperature. The PL properties of Eu ions in silicon nitride are different from those in SiAlON, which can be controlled by Al:Si ratio in starting materials. The morphological evolution of nitridation specimens was also affected by different starting materials. The products from pulverized coal furnace fly ash have a more obvious prismatic morphology. Meanwhile, the products from diatomite and raw illite show smaller particles and more fibers.

**Author Contributions:** Writing—Original draft, K.D.; Writing—Review and editing, C.W. and F.L.; formal analysis, K.D.; conceptualization, Y.J. and F.L.; data curation, K.D.; investigation, K.D.; resources, Y.J. and C.W.; project administration, Y.J. and B.X. All authors have read and agreed to the published version of the manuscript.

**Funding:** This research was funded by the National Natural Science Foundation of China (NSFC), grant No. 41702036 and grant No. 41472035.

**Acknowledgments:** Authors are grateful to editor and referees.

**Conflicts of Interest:** The authors declare no conflict of interest.

## References

1. Tanaka, I.; Nasu, S.; Adachi, H.; Miyamoto, Y.; Niihara, K. Electronic structure behind the mechanical properties of  $\beta$ -sialons. *Acta Metall. Mater.* **1992**, *40*, 1995–2001. [[CrossRef](#)]
2. Izhevskiy, V.A.; Genova, L.A.; Bressiani, J.C.; Aldinger, F. Progress in SiAlON ceramics. *J. Eur. Ceram. Soc.* **2000**, *20*, 2275–2295. [[CrossRef](#)]
3. Xie, R.J.; Hirosaki, N.; Mitomo, M.; Suehiro, T.; Xu, X.; Tanaka, H. Photoluminescence of rare-earth-doped Ca- $\alpha$ -SiAlON phosphors: Composition and concentration dependence. *J. Am. Ceram. Soc.* **2005**, *88*, 2883–2888. [[CrossRef](#)]
4. Xianqing, P.; Machida, K.; Horikawa, T.; Hanzawa, H. Synthesis and luminescent properties of low oxygen contained Eu<sup>2+</sup>-doped Ca- $\alpha$ -SiAlON phosphor from calcium cyanamide reduction. *J. Rare Earth* **2008**, *26*, 198–202.
5. Suehiro, T.; Onuma, H.; Hirosaki, N.; Xie, R.J.; Sato, T.; Miyamoto, A. Powder synthesis of Y- $\alpha$ -SiAlON and its potential as a phosphor host. *J. Phys. Chem. C* **2010**, *114*, 1337–1342. [[CrossRef](#)]
6. Ryu, J.H.; Park, Y.G.; Won, H.S.; Suzuki, H.; Kim, S.H.; Yoon, C. Luminescent properties of  $\beta$ -SiAlON: Eu<sup>2+</sup> green phosphors synthesized by gas pressured sintering. *J. Ceram. Soc. Jpn.* **2008**, *116*, 389–394. [[CrossRef](#)]
7. Ryu, J.H.; Won, H.S.; Park, Y.G.; Kim, S.H.; Song, W.Y.; Suzuki, H.; Yoon, C.B.; Kim, D.H.; Park, W.J.; Yoon, C. Photoluminescence of Ce<sup>3+</sup>-activated  $\beta$ -SiAlON blue phosphor for UV-LED. *Electrochem. Solid-State Lett.* **2010**, *13*, H30–H32. [[CrossRef](#)]
8. Wang, Z.; Ye, W.; Chu, I.H.; Ong, S.P. Elucidating structure-composition-property relationships of the  $\beta$ -SiAlON: Eu<sup>2+</sup> phosphor. *Chem. Mater.* **2016**, *28*, 8622–8630. [[CrossRef](#)]
9. Zhu, X.W.; Masubuchi, Y.; Motohashi, T.; Kikkawa, S. The z value dependence of photoluminescence in Eu<sup>2+</sup>-doped  $\beta$ -SiAlON (Si<sub>6-z</sub>Al<sub>z</sub>O<sub>z</sub>N<sub>8-z</sub>) with 1 ≤ z ≤ 4. *J. Alloy. Compd.* **2010**, *489*, 157–161. [[CrossRef](#)]
10. Ryu, J.H.; Park, Y.G.; Won, H.S.; Kim, S.H.; Suzuki, H.; Yoon, C. Luminescence properties of Eu<sup>2+</sup>-doped  $\beta$ -Si<sub>6-z</sub>Al<sub>z</sub>O<sub>z</sub>N<sub>8-z</sub> microcrystals fabricated by gas pressured reaction. *J. Cryst. Growth* **2009**, *311*, 878–882. [[CrossRef](#)]
11. Li, Y.Q.; Hirosaki, N.; Xie, R.J.; Takeda, T.; Mitomo, M. Crystal and electronic structures, luminescence properties of Eu<sup>2+</sup>-doped Si<sub>6-z</sub>Al<sub>z</sub>O<sub>z</sub>N<sub>8-z</sub> and M<sub>y</sub> Si<sub>6-z</sub>Al<sub>z-y</sub>O<sub>z+y</sub>N<sub>8-z-y</sub> (M = 2Li, Mg, Ca, Sr, Ba). *J. Solid State Chem.* **2008**, *181*, 3200–3210. [[CrossRef](#)]
12. Van Krevel, J.W.H.; van Rutten, J.W.T.; Mandal, H.; Hintzen, H.T.; Metselaar, R. Luminescence properties of terbium-, cerium-, or europium-doped  $\alpha$ -Sialon materials. *J. Solid State Chem.* **2002**, *165*, 19–24. [[CrossRef](#)]
13. Nekouee, K.A.; Khosroshahi, R.A. Preparation and characterization of  $\beta$ -SiAlON/TiN nanocomposites sintered by spark plasma sintering and pressureless sintering. *Mater. Des.* **2016**, *112*, 419–428. [[CrossRef](#)]
14. Jiang, P.; Wu, X.F.; Xue, W.D.; Chen, J.H.; Wang, W.; Li, Y. In-situ synthesis and reaction mechanism of  $\beta$ -SiAlON in the Al-Si<sub>3</sub>N<sub>4</sub>-Al<sub>2</sub>O<sub>3</sub> composite material. *Ceram. Int.* **2017**, *43*, 1335–1340. [[CrossRef](#)]
15. Yi, X.M.; Niu, J.; Nakamura, T.; Akiyama, T. Reaction mechanism for combustion synthesis of  $\beta$ -SiAlON by using Si, Al, and SiO<sub>2</sub> as raw materials. *J. Alloys Compd.* **2013**, *561*, 1–4. [[CrossRef](#)]
16. He, E.Q.; Yue, J.S.; Fan, L.; Wang, C.; Wang, H.J. Synthesis of single phase  $\beta$ -SiAlON ceramics by reaction-bonded sintering using Si and Al<sub>2</sub>O<sub>3</sub> as raw materials. *Scr. Mater.* **2011**, *65*, 155–158. [[CrossRef](#)]
17. Jun, K.; Lee, K.; Kim, G.; Kim, Y.J. A new route for the synthesis of  $\beta$ -sialon: Eu<sup>2+</sup> phosphors using pyrophyllite powders. *Ceram. Int.* **2013**, *39*, S349–S353. [[CrossRef](#)]
18. O’Leary, B.G.; MacKenzie, K.J.D. Inorganic polymers (geopolymers) as precursors for carbothermal reduction and nitridation (CRN) synthesis of SiAlON ceramics. *J. Eur. Ceram. Soc.* **2015**, *35*, 2755–2764. [[CrossRef](#)]
19. Bahramian, A.R.; Kokabi, M. Carbonitriding synthesis of  $\beta$ -SiAlON nanopowder from kaolinite–polyacrylamide precursor. *Appl. Clay Sci.* **2011**, *52*, 407–413. [[CrossRef](#)]

20. Tatlı, Z.; Demir, A.; Yılmaz, R.; Çalışkan, F.; Kurt, A.O. Effects of processing parameters on the production of  $\beta$ -SiAlON powder from kaolinite. *J. Eur. Ceram. Soc.* **2007**, *27*, 743–747. [[CrossRef](#)]
21. Kudyba-Jansen, A.A.; Hintzen, H.T.; Metselaar, R. Ca- $\alpha/\beta$ -sialon ceramics synthesised from fly ash-preparation, characterization and properties. *Mater. Res. Bull.* **2001**, *36*, 1215–1230. [[CrossRef](#)]
22. Zhao, H.; Wang, P.Y.; Yu, J.L.; Zhang, J. A mechanistic study on the synthesis of  $\beta$ -Sialon whiskers from coal fly ash. *Mater. Res. Bull.* **2015**, *65*, 47–52. [[CrossRef](#)]
23. Ma, B.Y.; Li, Y.; Yan, C.; Ding, Y.S. Effects of synthesis temperature and raw materials composition on preparation of  $\beta$ -Sialon based composites from fly ash. *Trans. Nonferr. Met. Soc. China* **2012**, *22*, 129–133. [[CrossRef](#)]
24. Gilbert, J.E.; Mosset, A. Preparation of  $\beta$ -SiAlON from fly ashes. *Mater. Res. Bull.* **1998**, *33*, 117–123. [[CrossRef](#)]
25. Dou, K.Z.; Jiang, Y.S.; Xue, B.; Wei, C.D.; Li, F.F. The carbon environment effects on phase composition and photoluminescence properties of  $\beta$ -SiAlON multiphase materials prepared from fly ash acid slag. *Ceram. Int.* **2019**, *45*, 7850–7856. [[CrossRef](#)]
26. Seidel, A.; Sluszný, A.; Shelef, G.; Zimmels, Y. Self inhibition of aluminum leaching from coal fly ash by sulfuric acid. *Chem. Eng. J.* **1999**, *72*, 195–207. [[CrossRef](#)]
27. Matjie, R.H.; Bunt, J.R.; van Heerden, J.H.P. Extraction of alumina from coal fly ash generated from a selected low rank bituminous South African coal. *Miner. Eng.* **2005**, *18*, 299–310. [[CrossRef](#)]
28. Jiang, T.; Xue, X.X.; Duan, P.N.; Liu, X.; Zhang, S.H.; Liu, R. Carbothermal reduction–nitridation of titania-bearing blast furnace slag. *Ceram. Int.* **2008**, *34*, 1643–1651. [[CrossRef](#)]
29. Tang, Y.; Yin, H.F.; Yuan, H.D.; Shuai, H.; Xin, Y.L. Carbothermal reduction nitridation of slag, glass and minerals: Formation process of SiAlON powders with different morphology. *Ceram. Int.* **2016**, *42*, 7499–7505. [[CrossRef](#)]
30. Hotta, M.; Tatami, J.; Zhang, C.; Komeya, K.; Meguro, T.; Terner, M.R.; Cheng, Y.B. Ca- $\alpha$  SiAlON hollow spheres prepared by carbothermal reduction–nitridation from different SiO<sub>2</sub> powders. *Ceram. Int.* **2010**, *36*, 1553–1559. [[CrossRef](#)]
31. Panda, P.K.; Mariappan, L.; Kannan, T.S. Carbothermal reduction of kaolinite under nitrogen atmosphere. *Ceram. Int.* **2000**, *26*, 455–461. [[CrossRef](#)]
32. Antsiferov, V.N.; Gilyov, V.G.; Karmanov, V.I. IR-spectra and phases structure of sialons. *Vib. Spectrosc.* **2002**, *30*, 169–173. [[CrossRef](#)]
33. Wang, F.; Jin, G.; Guo, X. Formation Mechanism of Si<sub>3</sub>N<sub>4</sub> Nanowires via Carbothermal Reduction of Carbonaceous Silica Xerogels. *J. Phys. Chem. B* **2006**, *110*, 14546–14549. [[CrossRef](#)] [[PubMed](#)]
34. Yariv, S.; Lapidés, I.; Nasser, A.; Lahav, N.; Brodsky, I.; Michaelian, K.H. Infrared study of the intercalation of potassium halides in kaolinite. *Clays Clay Miner.* **2000**, *48*, 10–18. [[CrossRef](#)]
35. Yu, F.; Yang, J.; Delsing, A.; Hintzen, B. Preparation, characterization and luminescence properties of porous Si<sub>3</sub>N<sub>4</sub> ceramics with Eu<sub>2</sub>O<sub>3</sub> as sintering additive. *J. Lumin.* **2010**, *130*, 2298–2304. [[CrossRef](#)]

